

Simulating Antihydrogen Annihilation Distributions in ASACUSA's Cusp Trap

Alison Weiss

CERN Summer Student Program, 2022

Advisor: Dr. Eric Hunter

1 Abstract

The hyperfine structure of hydrogen is known very precisely, and if charge, parity and time reversal (CPT) symmetry holds, antihydrogen will have the exact same spectrum. CPT violation may help explain the baryon asymmetry, the mysterious and presently unexplained fact that the universe contains much more matter than antimatter.⁶ The Atomic Spectroscopy And Collisions Using Slow Antiprotons (ASACUSA) Collaboration aims to measure the ground state hyperfine structure of antihydrogen in a magnetic field-free region with a precision of 1 ppm.⁵ Antiproton and positron plasmas, which are produced further upstream, are combined in the Cusp trap.³ We use SIMION to simulate antihydrogen trajectories in the spatially varying magnetic field of ASACUSA's Cusp trap.¹ We use the resulting annihilation distributions as a look-up table in a Python routine which accounts for plasma rotation and thermal velocity distribution. This work allows us to evaluate the antihydrogen ground state annihilation distributions for ranges of plasma properties, helping us to optimize antihydrogen production.

2 ASACUSA's Cusp Trap

Antihydrogen is produced in the Cusp trap, which is comprised of superconducting anti-Helmholtz coils and multiple ring electrodes. Positron and antiproton plasmas that are produced further upstream in the ASACUSA experimental apparatus are combined in the Cusp trap, a process called mixing. Cusp magnets then guide low field seeking antihydrogen downstream while rejecting high field seeking antihydrogen to form a spin-polarized beam. In order to make the measurement, low field seeking antihydrogen must reach the BGO (Bi₄Ge₃O₁₂) scintillator disk, which is our antihydrogen detector.⁴

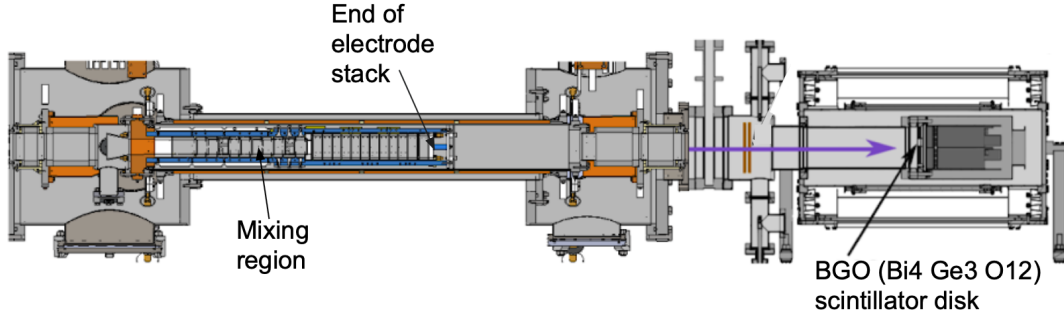


Figure 1: CAD diagram of ASACUSA's Cusp trap.

3 Simulation Methods

We modeled the Cusp trap with C++ and input the model into SIMION to simulate the antihydrogen trajectories.

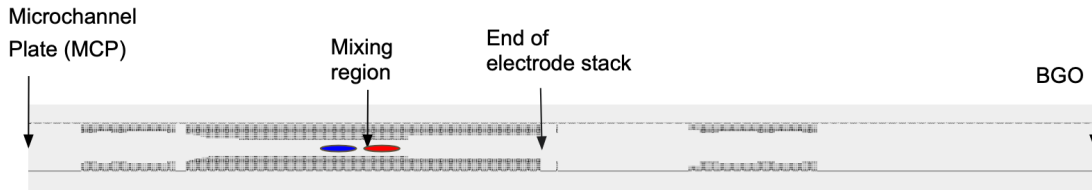


Figure 2: The outline of the Cusp trap used in our SIMION annihilation trajectory calculations. The red ellipse represents the positron plasma and the blue ellipse represents the antiproton plasma.

Only a small fraction of formed antihydrogen have the correct initial velocity to reach the BGO, as only antihydrogen with velocities directed within about 6 degrees of the Cusp's axis will be guided through the trap. Antihydrogen with velocities further off axis will hit the walls of the trap and annihilate before reaching the BGO.

The thermal velocities of the antihydrogen are assumed to be isotropically distributed, with no preference for a particular direction. However, since the positron plasma is rotating, antihydrogen formed off-axis will have a transverse velocity component proportional to the radial distance from the axis and the rotational frequency.

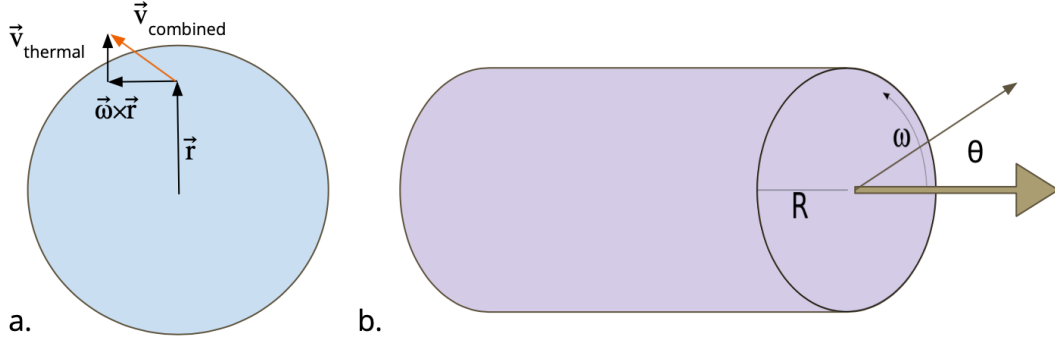


Figure 3: Panel (a): a diagram of the plasma’s cross section, showing the velocity vector addition of antihydrogen formed a distance r off-axis in a plasma rotating at angular frequency ω . Panel (b): a diagram of a plasma rotating at angular frequency ω . The thermal velocity is directed at an angle θ above the trap’s axis.

To account for this effect, we wrote a program in Python which sums the formed antihydrogen’s thermal and rotational velocities and outputs a combined velocity. We then use the array output from SIMION as a look-up table to extract the annihilation positions for the antihydrogen given their combined initial velocity and magnetic moment.

We restrict our simulations to the ground state for two reasons. First, our hyperfine measurement will be of ground state antiatoms, so we are most interested in their behavior for optimizing our plasma properties. Second, the simulations are quantum mechanically complicated for excited states. The ℓ states are degenerate, so the antiatoms’ energies change as a function of the magnetic field and must be determined by degenerate perturbation theory calculations.² The diamagnetic effect changes the magnetic force on the antihydrogen, and thus alters the antiatom’s trajectories through the trap. We can neglect the diamagnetic term for the ground state, but it will need to be included to accurately simulate excited states.

4 Plasma Properties

We can experimentally tune several of the positron plasma’s properties: the rotational frequency, the radial thickness and the temperature. The rotational frequency is proportional to the plasma’s density. A higher density means that antiatoms will not travel as far before re-ionizing and are more likely to become tightly bound before reaching a higher radius. Thus, denser plasmas have smaller formation regions. However, a higher frequency means an increased centrifugal effect. A larger radial thickness allows for some antihydrogen to be formed at higher radii, but it also means that antiatoms will spend more time in the plasma and will thus be more likely to be de-excited to the ground state. As for temperature, lower is better, since the focusing of our Cusp magnets is better and de-excitation proceeds faster.

5 Results

5.1 Ground State Annihilation Distributions

Key features from the Cusp trap are visible in our annihilation distributions.

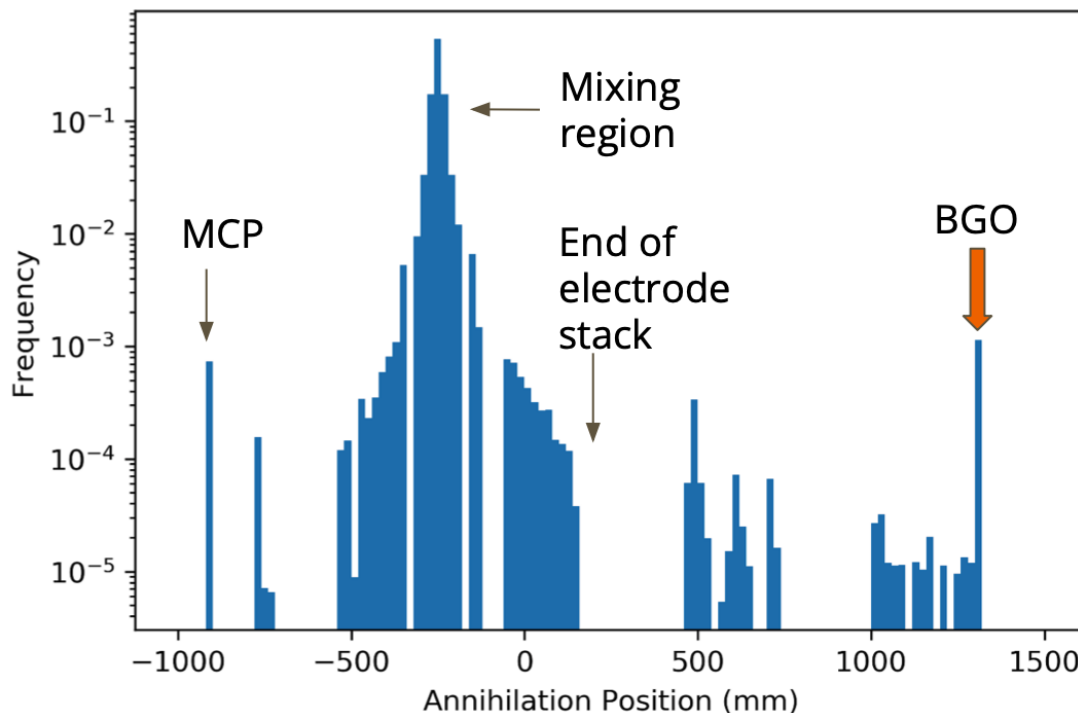


Figure 4: Plot showing the annihilation distribution for ground state low field seekers formed 0.1 mm away from the axis in a 20 K plasma which is rotating at 100 kHz. Antihydrogen energies are Maxwellian distributed. A 0.1 mm radius’s achievability is uncertain, as it depends on the formation rate and re-ionization diffusion. 20 K, while a very low temperature, should be achievable with evaporative cooling. 100 kHz is within the range of accessible frequencies using the strong drive regime rotating wall technique. The x-axis is the annihilation position along the trap, with zero being the midpoint between the two field nulls of the Cusp magnet.

Most antihydrogen annihilate near the mixing region, but some make it through to the BGO. We see a gap in annihilations at the end of the electrode stack. This is due to the geometry of the trap. When the trap widens, antiatoms that made it through the narrower region do not have velocities such that they will annihilate early in the wider region.

5.2 Initial Antihydrogen Velocities

It turns out that most of the particles that reach the BGO did not have initial thermal velocity within the ± 6 degree slice that reaches the BGO. Most particles who make it down the trap to the BGO were “kicked” into the range of acceptable velocities by the plasma’s rotation. This effect is significant even at small radii.

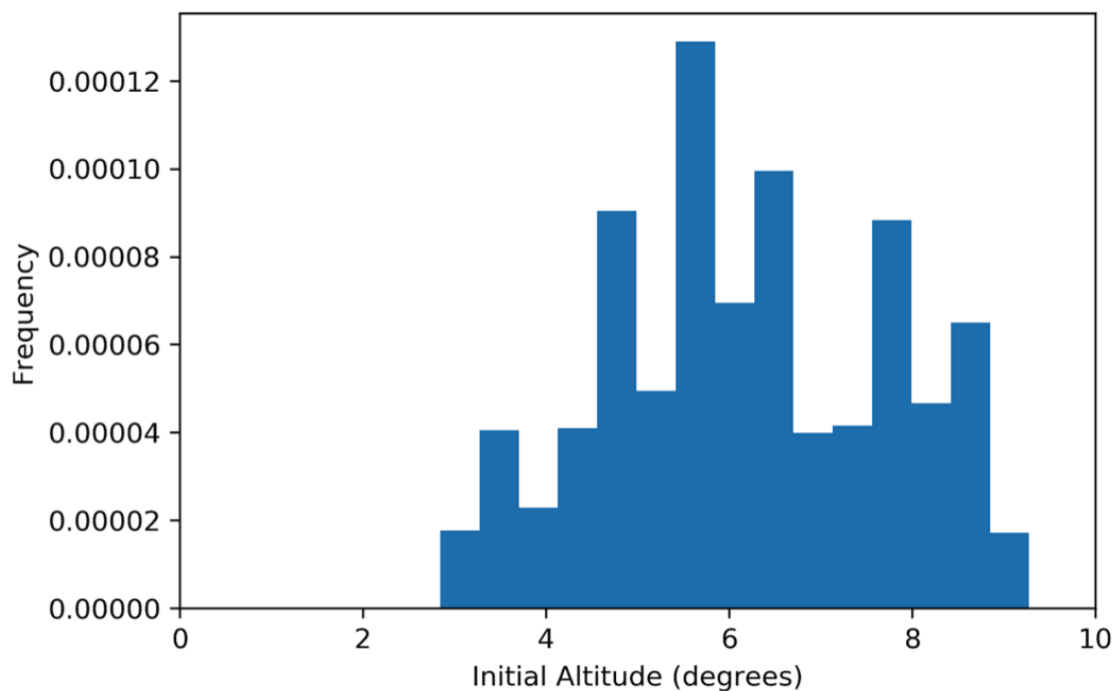


Figure 5: Plot showing the frequency of initial altitudes of the thermal velocities for antihydrogen that reached the BGO. The antihydrogen had initial energy of 0.0018 eV and originated at a radius of 0.1 mm in a plasma rotating at 100 kHz.

In Figure 5, we see that for antihydrogen with 0.0018 eV of initial energy formed at a radius of 0.1 mm in a plasma rotating at 100 kHz, no antihydrogen with their initial thermal velocity directed down the trap reach the BGO. Those antihydrogen seem to have been “kicked” out of the acceptable range of velocities by the plasma’s rotation, while the antihydrogen who do reach the BGO were “kicked” in.

Since particles with thermal velocity pointing farther from the axis occupy a larger fraction of the solid angle, this effect likely makes the radial drop-off in fraction of particles reaching the BGO less severe than expected.

5.3 Sweeping Tunable Plasma Properties

We study how the fraction of antihydrogen reaching the BGO is affected by varying our tunable parameters: radius, frequency and temperature.

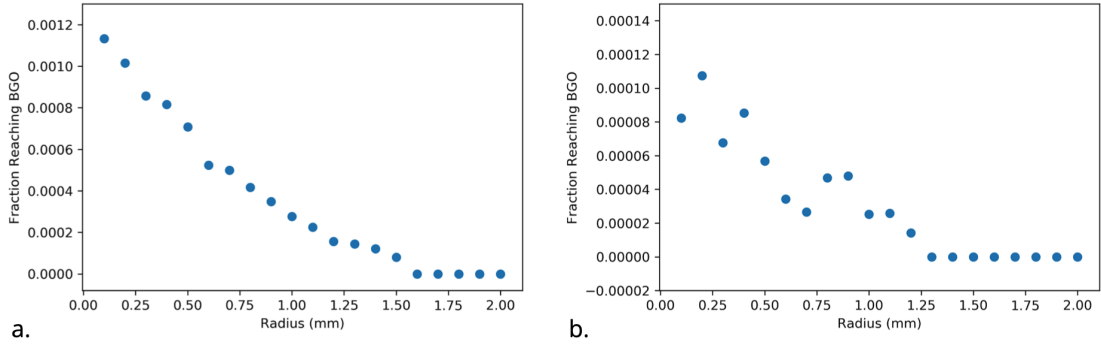


Figure 6: Panel (a): plot showing the fraction of ground state low field seeking antihydrogen from a 20K plasma rotating at 100 kHz that reach the BGO as a function of the formation radius. Panel (b): the same but for high field seeking antihydrogen. The ‘noise’ visible in these plots is thought to be an artifact from the discretization of the rotational angle and the initial thermal velocity.

At high enough radii, the rotational effect is so large that it “kicks” all antihydrogen to the walls of the trap near the formation region, so none make it to the BGO. At lower radii, we see an order of magnitude more low field seekers than high field seekers, due to the Cusp magnets’ focusing of low field seekers and rejection of high field seekers.

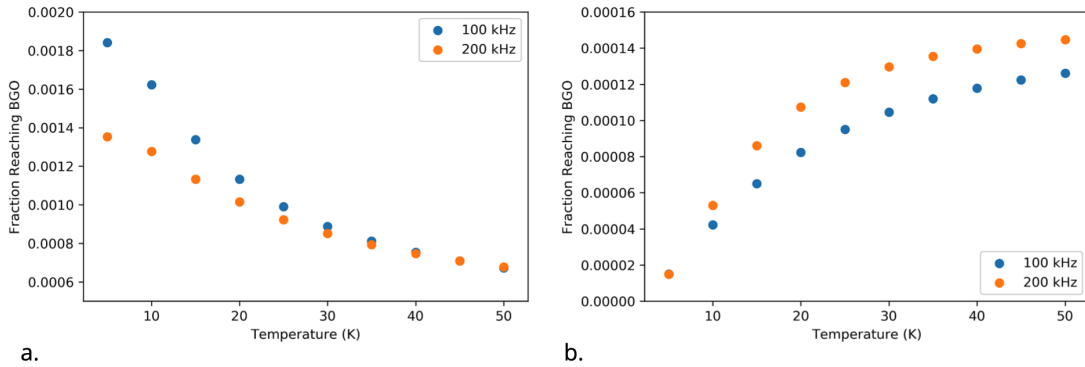


Figure 7: Panel (a): plot showing the fraction of ground state low field seeking antihydrogen formed at a radius of 0.1 mm that reach the BGO as a function of the plasma temperature. Blue dots correspond to a plasma rotational frequency of 100 kHz and orange dots correspond to a frequency of 200 kHz. Panel (b): the same but for high field seeking antihydrogen.

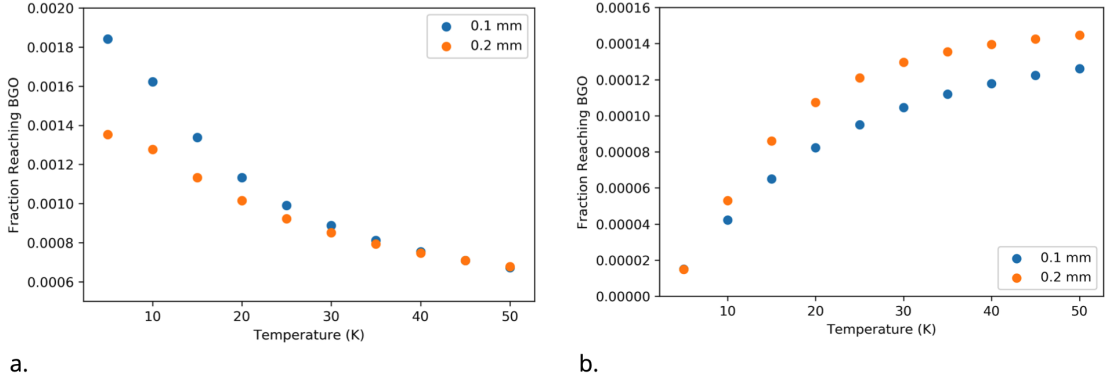


Figure 8: Panel (a): plot showing the fraction of ground state low field seeking antihydrogen formed in a plasma rotating at 100 kHz as a function of plasma temperature. Blue dots represent antihydrogen forming at a radius of 0.1 mm and orange dots represent antihydrogen forming at a radius of 0.2 mm. Panel (b): the same but for high field seeking antihydrogen.

Our results confirm that lower temperatures are better for both focusing low field seeking antiatoms and rejecting high field seekers. Also notice that doubling the radius has the same effect as doubling the frequency, since the rotational “kick” is proportional to both frequency and radius.

6 Future Work

To continue with this project, we must properly account for the diamagnetic effect using degenerate perturbation theory to properly calculate the trajectories for high quantum numbers. Doing so will allow us to include excited states in our simulations and ultimately predict the full annihilation distribution as detected by our Brescia panel detectors.

It will also be valuable to calculate the expected time each antihydrogen spends in the plasma as this relates to de-excitation likelihood.

7 Acknowledgements

I want to thank Dr. Eric Hunter and Andreas Lanz for their guidance and many helpful explanations this summer. I would also like to thank the National Science Foundation and the University of Michigan CERN REU program for supporting me. In particular, I want to thank Myron Campbell, Junjie Zhu and Steve Goldfarb. I also want to thank the CERN Summer Student Program organizers for all their work to make this experience possible.

References

- ¹ Dahl, D. A. SIMION 3D Version 7.0 User's manual, 2000.
- ² Gallagher, T. *Rydberg Atoms*. Cambridge: Cambridge University Press, 1994.
- ³ Hunter, E.D. et al. Minimizing plasma temperature for antimatter mixing experiments. *EPJ Web Conf.*, 262:01007, 2022. [doi:10.1051/epjconf/202226201007](https://doi.org/10.1051/epjconf/202226201007).
- ⁴ Kuroda, N., Ulmer, S., Murtagh, D.J. et al. The ASACUSA CUSP: an antihydrogen experiment. *Hyperfine Interact*, 235:13–20, 2015. [doi:10.1007/s10751-015-1205-1](https://doi.org/10.1007/s10751-015-1205-1).
- ⁵ Malbrunot, C. et al. The ASACUSA antihydrogen and hydrogen program: results and prospects. *Philosophical Transactions of the Royal Society A: Mathematical, Physical and Engineering Sciences*, 376(2116):20170273, 2018. [doi:10.1098/rsta.2017.0273](https://doi.org/10.1098/rsta.2017.0273).
- ⁶ Sakharov, A.D. Violation of CP-Invariance, C-Asymmetry, and Baryon Asymmetry of the Universe. Translated from *Zhurnal Eksperimental'noi i Teoreticheskoi Fiziki: Pis'ma v Redaktsiyu*. 5:32–35, 1967. [doi:10.1142/9789812815941_0013](https://doi.org/10.1142/9789812815941_0013).